Recibido: 5 de febrero 2019 Aceptado: 28 de Agosto 2019

Exergy analysis of a solar heating and cooling system that uses phase change materials. PCMSOL Project

Análisis de exergía de un sistema solar de calentamiento y enfriamiento que utiliza materiales de cambio de fase. Proyecto PCMSOL

Diana Maldonado[1], Marcos Luján[1], Sabina Rosiek[2], Javier Batlles[2], Svetlana Ushak[3]

[1]Universidad Católica Boliviana San Pablo, Departamento de Ciencias Exactas, c Márquez s/n, Campus Tupuraya, Cochabamba, Bolivia
[2]Universidad de Almería, Departamento de Física Aplicada, 04120 Almería, España
[3]Universidad de Antofagasta, Departamento de Ingeniería Química y Procesamiento de minerales, Campus Coloso, Antofagasta, Chile

diana.mc.519@gmail.com

Resumen: El presente trabajo está basado en la aplicación de un análisis de exergía al sistema de calefacción y refrigeración solar (específicamente en modo de refrigeración) actualmente implementado en el Centro de Investigación de Energía Solar CIESOL de la Universidad de Almería (España), con el fin de poder determinar un sistema más eficiente y evaluar el efecto de la introducción de materiales de cambio de fase (PCMs) al sistema de climatización. El análisis realizado dio como resultado que dicho sistema solar actual alcanza una eficiencia exergética máxima global de tan solo 6.6%, y que la introducción de los PCMs logra aumentar las capacidades de almacenamiento térmico del sistema, sin embargo, provoca una mínima disminución en la eficiencia exergética global a 6.5%. Así también, los resultados mostraron que, a diferencia de lo que refleja un análisis energético, los componentes que mayores irreversibilidades generan son los colectores solares, con casi el 90% de pérdidas del total captado. Consecuentemente, se realizó una propuesta de reducción de las irreversibilidades generadas por los componentes solares del sistema de climatización solar, incorporando el uso de paneles fotovoltaicos en vez de los colectores solares, esto mejora la eficiencia exergética global del sistema.

Palabras clave: Sistema de refrigeración; Energía solar; Análisis de exergía; Irreversibilidades; almacenamiento térmico; materiales de cambio de fase.

Abstract: The present work is based on the application of an exergy analysis to the solar-assisted heating and cooling system (specifically in cooling mode) currently installed at the CIESOL Solar Energy Research Center of the Almeria University (Spain); in order to determine a more efficient system and to evaluate the effect of the phase change materials (PCMs) introduction into the heating and cooling systems. The analysis shows that the current solar system achieves an overall maximum exergy efficiency of 6.6%. In addition, the introduction of the PCMs manages to increase the thermal storage capacities of the system, however, it causes a slight decrease in the global exergy efficiency to 6.5%. The results also show that, unlike what an energy analysis reflects, the components that generate the greatest irreversibilities are the solar collectors, with almost 90% of the total exergy losses. Consequently, a proposal was made to reduce the irreversibilities generated by the solar thermal components of the system, incorporating the use of photovoltaic panels instead of solar collectors, this improves the overall exergy efficiency.

Key words: Heating and cooling system; solar energy; exergy analysis; irreversibilities; thermal storage; phase change materials

Nomenclature

A	Opening area of solar collectors (m^2)	0	Ambient, ambient of reference
Cp	Specific heat ($kJ \cdot kg^{-1} \cdot K^{-1}$)	1*	Collector output/ initial state
E	Energy (kJ)	2*	Hot storage tank output/ final state
$\dot{E}$	Energetic flux ($kJ \cdot s^{-1}$)	3	Collector input
Ex	Exergy (kJ)	4	Generator input
$\dot{E}x$	Exergy flux ($kJ \cdot s^{-1}$)	5	Generator output
H	Enthalpy (kJ)	6	Cooling tower output
ΔH	Fusion enthalpy ($kJ \cdot kg^{-1}$)	7	Cooling tower conduit
h	Specific enthalpy ($kJ \cdot kg^{-1}$)	8	Cooling tower conduit
I	Irreversibilities (kJ)	9	Cooling tower input
$\dot{I}$	Irreversibilities flux ($kJ \cdot s^{-1}$)	10	Evaporator input
I_s	Solar irradiance ($W \cdot m^{-2}$)	11	Evaporator output
m	Mass (kg)	12	Cold storage tank output
$\dot{m}$	Mass flux ($kg \cdot s^{-1}$)	13	Chilled water entrance
P	Pressure (kPa)	14	Absorber output
Q	Heat transfer (kJ)	15	Heat exchanger input
$\dot{Q}$	Heat transfer flux ($kJ \cdot s^{-1}$)	16	Generator input
s	Specific entropy ($kJ \cdot kg^{-1} \cdot K^{-1}$)	17	Generator output
S	Entropy ($kJ \cdot K^{-1}$)	18	Heat exchanger output
$\dot{S}$	Entropy flux ($kJ \cdot s^{-1} \cdot K^{-1}$)	19	Absorber input
T	Temperature (°C or K)	20	Condenser input
UA	Heat transfer coefficient ($W \cdot {}^{\circ}C^{-1}$)	21	Condenser output
W	Work (kJ)	22	Evaporator input
$\dot{W}$	Work flux ($kJ \cdot s^{-1}$)	23	Evaporator output

X	Mass fraction (dimensionless)
η	Energetic performance (Fist Law – dimensionless)
ψ	Exergetic availability (kJ·kg^{-1})
ε_{sun}	Specific exergetic sun availability (kJ·kg^{-1})
ρ	Density (kg·m^{-3})
ξ	Exergy efficiency (Second Law – dimensionless)
Φ	Exergetic mass availability (kJ·kg^{-1})

Main abbreviations

SHC	Solar Heating and Cooling
PCM	Phase Change Material

1 Introduction

The domestic energy consumption is one of the sectors with the highest energy consumption in the world; therefore, important attention should be given to this area. Ventilation, residential heating, air-conditioning (HVAC) and hot water production accounts for about 60% of the energy consumed in the U.S. homes [1] [2]. These values reflect that, despite the importance given to the electric consumption reduction and the implementation of efficient electrical equipment, there is a great demand for thermal energy. Consequently, the air conditioning area represents a great opportunity to reduce the energy consumption in buildings, to improve energy security and reduce CO_2 emissions [3].

In the field of air conditioning, solar energy is used not only to generate heating but also to generate cooling. Two of the most common options in domestic and public applications are solar thermal cooling and solar electric cooling. The first one is based on thermal solar systems that transfer heat in order to operate absorption cooling cycles, which generate cold through the evaporation of the refrigerant at low pressures [4]. In electric refrigeration, photovoltaic panels are commonly used to generate electricity and operate a refrigeration cycle equipment [5]. During the winter or cold season, the heat or electricity produced by the solar thermal collectors or PV panels can be used either to provide hot water or electrical power to a corresponding equipment [4].

In terms of systems' analysis, the second law efficiency analysis or the exergy analysis is considered one of the most reliable tools for the analysis of thermodynamic processes [6], where the exergy (or availability) of a closed system in a determined state, is defined as the maximum useful work that can be obtained from a system-environment combination. The exergy analysis is used strategically in the design, simulation and performance evaluation of systems and their components [6] [7]. In other words, this second law analysis can determine the quantitative magnitude of exergy losses (or irreversibilities) associated with a system or process. Therefore, it provides a criteria to know the ways in which the performance can be improved and to reduce operating costs of these thermodynamic systems [8].

The present work is part of the PCMSOL project, or "Thermal Energy Storage with Phase Change Materials for Solar Cooling and Heating Applications: A technology viability analysis", led by the Almería University (UAL) and funded by the ERANeT-LAC. The PCMSOL project approach is to develop and test new phase change materials (PCM) that can be integrated into thermal energy storage units (STES) as part of the solar heating and cooling (SHC) system currently installed in Almeria [8]. Therefore, the overall aim is to search for the best available PCMs locally, compare their performance with current water storage systems, verify the most appropriate STES tank size and mainly determine the current and future efficiency of the SHC system.

The scope of this article covers the analysis of the SHC system proposed in the framework of the PMCSOL project in cooling mode, using a basic methodology for the identification of locations with greater losses of exergy, based on the second law of thermodynamics or the generation of entropy and the relationship with its environment. This methodology is adaptable to the thermodynamic analysis of any thermal machine, encompassing air conditioning in general. The resulting exergy efficiency analysis, as well as the identification of irreversibilities of the system, will allow a better use of the energy resources of the system, consequently selecting a more viable proposal in energy terms.

2 Methodology

A scheme referring to the Solar Heating and Cooling (SHC) system currently installed at the CIESOL center was used (Figure 1:), as well as the scheme of the internal components that represents the absorption equipment (Figure 2:) used in the generation of cold.

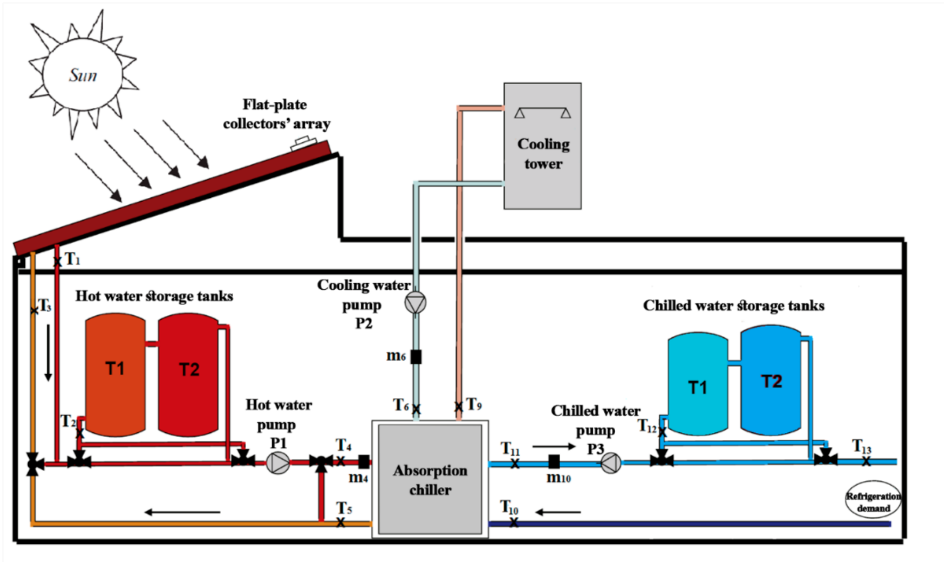

Figure 1: General scheme of the SHC installed in CIESOL, drawn based on Rosiek & Batlles [9]

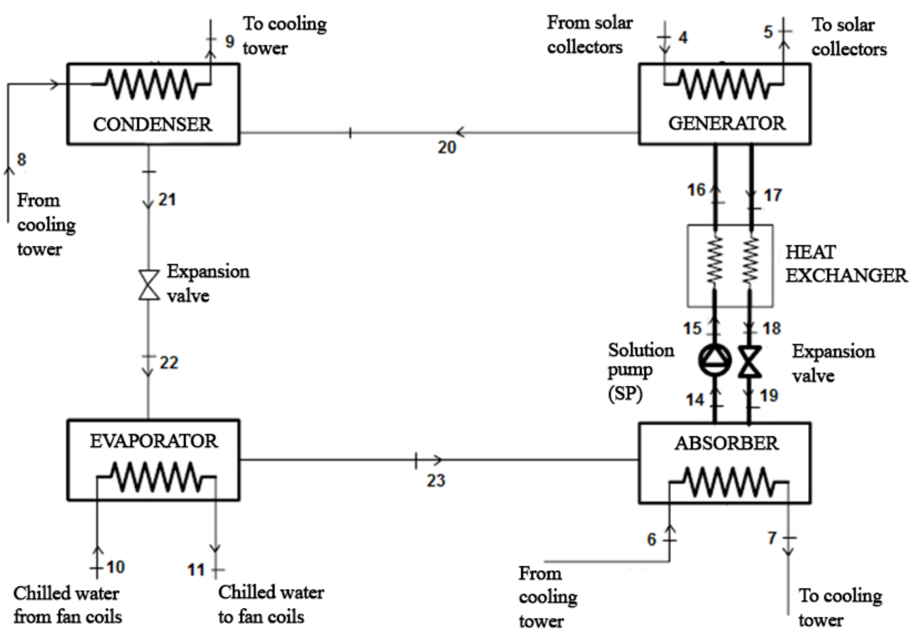

Figure 2: General scheme of the absorption chiller, drawn based on Zadeh & Bozorgan [10]

Both diagrams are intended to facilitate the global understanding of the entire SHC system under cooling mode, as well as to determine the thermodynamic states of each input and output flow of all system components. Within the integrated components of the SHC system (Figure 1:Figure 2:), they were considered as the most representative control volumes of the system, which allowed the global exergy and energy analysis. Moreover, special emphasis was given to the absorption chiller and its internal components: generator, heat exchanger, absorber, evaporator and condenser (Figure 2:).

In order to identify the operation mode of the equipment and components of the SHC system installed in the CIESOL center, a bibliographic review of all the information published by the researchers of the center was carried out, as well as the revision of the datasheets of each equipment. It was fundamental to have a thorough knowledge of all the equipment and components of the system, considering characteristics such as: size, capacity, optimal temperature ranges of entry and exit, performance, among others.

The PVGIS platform or Photovoltaic Geographical Information System was used [11] to determine the solar radiation captured by the solar collectors in the study area. In this section, the total area covered by the collectors was considered (160 m^2), as well as the inclination value of them (30°), and the data of the months of low, medium and high solar radiation within the summer season were selected. In the case of the reference ambient temperature of the study area, it was obtained through the State Meteorological Agency (AEMet) [12] and the Agroclimatic Information System for Irrigation (SiAR) [13].

The identification of the cold demand plays a fundamental role for the analysis of the SHC system, since the functioning and the inputs and outputs flows of the components of the entire system depend on it. In order to execute the analysis under periods of high, medium and low solar radiation, average hourly values were used for the months of May, August and September, based on the data and results available in the CIESOL solar investigation center.

Regarding the application of the exergy analysis, the input and output flows determined by each system control volume were used. It must be mentioned that, in order to apply the analysis of second law, the first law corresponding to energy flow balances must first be complied with [14]. Each inflow and outflow were considered a control point; therefore, it was necessary to determine its thermodynamic properties according to the following table.

Table 1: Thermodynamic properties by inflows and outflows [14]

N°	Variable	Symbol	SI
1	State	-	-
2	Solution	-	-
3	LiBr fraction	$X_{(LiBr)}$	[%]
4	Temperature	T	[°C]
5	Pressure	P	[kPa]
6	Mass flow	$\dot{m}$	[$kg\cdot s^{-1}$]
7	Enthalpy	h	[$kJ\cdot kg^{-1}$]
8	Entropy	s	[$kJ\cdot kg^{-1}\cdot K^{-1}$]
9	Quality	-	-

For the energy balance of the solar collector, a reference was made to Cabrera & Gil [15], who use the following equation for the analysis of flat-plate solar collectors.

$$\dot{E}_{sun} = I_S \cdot A \cdot n_{plates} \quad \text{(Ec. 1)}$$

$$\dot{Q}_{sc} = \eta_{sc} \cdot I_S \cdot A \cdot n_{plates} \quad \text{(Ec. 2)}$$

Where, $\dot{E}_{sun}$ corresponds to the amount of radiant energy received by the solar collectors, I_S to the solar radiation corresponding to the inclination surface and the location, A is the opening area of the solar collectors and finally n_{plates} is the number of flat-plates solar collectors installed. The last two variables belong to the physical and installation characteristics of the CIESOL solar collectors. $\dot{Q}_{sc}$ represents the amount of energy transferred by the solar collector to the heat transfer fluid circulating through them (in this case water), and finally η corresponds to the design performance of the collectors and is obtained through the following equation [16], where T_m and T_0 are the mean temperature of the fluid and ambient temperature, respectively.

$$\eta_{sc} = \eta_o - \left[a_1\left(\frac{T_{m,sc} - T_o}{I_S}\right) - a_2\frac{\left(T_{m,sc} - T_o\right)^2}{I_S}\right] \quad \text{(Ec. 3)}$$

In the case of the heat and cold storage tanks, equation 4 was applied, in order to be able to determine the delivery or reserve of thermal energy by them. In this case, the transfer heat to the environment generated by the isolation characteristics of the reserve tanks was taken into account. For both tanks the heat transfer coefficient (UA) was considered as R16, equivalent to 5.7605 [W $°C^{-1}$].

$$\int_1^2 -Q_{UA}dt = \int_1^2 dH_{V.C} + \int_1^2 (h_{out} - h_{in}) \cdot dm \qquad \text{(Ec. 4)}$$

The development of the above equation derives in equations 5 and 6, which refer to the energy stored in the heat and cold reserve system tanks, with (Ec. 6) and without (Ec. 5) the use of phase change materials (PCMs).

$$\begin{aligned} Q_{storage} = {} & M_{H_2O}\left(h_{2,tc} - h_{1,tc}\right) \\ & = (h_1 - h_2)\, m_1 - UA(T_{m,tc} - T_o) \end{aligned} \qquad \text{(Ec. 5)}$$

$$\begin{aligned} Q_{storage} = {} & M_{H_2O}\left(h_{2,tc} - h_{1,tc}\right) + M_{PCM}\left(h_{2,PCM} - h_{1,PCM}\right) \\ & = (h_1 - h_2)\, m_1 - UA(T_{m,tc} - T_o) \end{aligned} \qquad \text{(Ec. 6)}$$

Now, the most complex case of the system under analysis corresponds to the absorption chiller, which has five internal components: generator, condenser, evaporator, absorber and heat exchanger, and each of them was considered as a single control volume within the whole system.

Based on the energy and exergy analyzes for the single-effect LiBr absorption chiller performed by Kalogirou [17] and Zadeh & Bozorgan [10], the following equations were used to determine the energy balances of each absorption chiller's components.

$$\dot{m}_{LiBr\ concentrated} X_{LiBr\ concentrated} = \dot{m}_{LiBr\ dilute} X_{LiBr\ dilute} \qquad \text{(Ec. 7)}$$

$$\dot{m}_{LiBr\ dilute} = \dot{m}_{LiBr\ concentrated} + \dot{m}_{refrigerant} \qquad \text{(Ec. 8)}$$

$$\dot{Q} + \dot{W}_f = \sum h_{out}\dot{m}_{out} - \sum h_{in}\dot{m}_{in} \qquad \text{(Ec. 9)}$$

For the exergy balances application, it started with the calculation of the exergetic solar radiation available in the study area, using the following equation [18]:

$$\varepsilon_{sun,max} = 1 + \frac{1}{3}\left(\frac{T_0}{T_{sr}}\right)^4 - \frac{4}{3}\left(\frac{T_0}{T_{sr}}\right) \qquad \text{(Ec. 10)}$$

Where, T_{sr} is equal to the temperature of the sun's surface and corresponds to a fixed value of 6,000 K. The radiant exergy that enters the solar collectors was calculated according to Hepbasli [6], where *A* corresponds to the opening area of the solar collectors. and $\boldsymbol{\varepsilon}_{sun}$ reflects the exergetic availability of solar radiation, previously calculated.

$$Ex_{radiant} = A \cdot n_{cs} \cdot I_s \cdot \varepsilon_{sun} \qquad \text{(Ec. 11)}$$

Now, the application of the exergy balance to a well-defined control volume was made following the Wark & Richards [14] equation:

$$\dot{W}_{f,real} - \dot{W}_{f,optimum} = \dot{I} \qquad \text{(Ec. 12)}$$

Where, the $W_{f,real}$ corresponds to the real work exchanged with the system, $W_{f,optimum}$ is the reversible or optimum work that would be exchanged, I corresponds to the amount of exergy destroyed by the system (Ex_{des},). $W_{f,optimum}$ is calculated as follows:

$$\delta W_{f,optimum} = d\Phi_{C.V.} + \sum \psi_{out} dm_{out} - \sum \psi_{in} dm_{in} + \sum \left(1 - \frac{T_o}{T_k}\right) \cdot \delta Q_k \qquad \text{(Ec. 13)}$$

or

$$\delta W_{f,optimum} = d\Phi_{C.V.} + \sum \psi_{out} dm_{out} - \sum \psi_{in} dm_{in} + \sum \left(\frac{T_o - T_{kf}}{T_{kf}}\right) \cdot \delta Q_{kf} \qquad \text{(Ec. 14)}$$

For systems below the ambient temperatures. Where, Φ refers to the exergetic mass availability, the ψ to the exergetic availability and Q to the heat transfer.

The exergy content is expressed by unit of mass, as follows:

$$\psi = (h - h_0) - T_0(s - s_0) + \frac{V^2}{2} + gz \qquad \text{(Ec. 15)}$$

Where *h* is the specific enthalpy, *s* is the specific entropy, and the zero subscript indicates the properties of the system at strict dead state in equilibrium with the environment. The two last parts of the equations correspond to the specific kinetic and potential energy.

For adiabatic systems, the transfer of exergy through heat is equal to zero. In real processes, irreversibilities occur and as a result, there is entropy generation, which results in the destruction of a specific amount of exergy that can be calculated with the Gouy-Stodola equation [6].

$$\dot{I} = \dot{E}x_{destroyed} = T_o \dot{S}_{universe} \geq 0 \qquad \text{(Ec. 16)}$$

According to Wark & Richards [14], the entropy generated by the universe can be found by means of the following equation:

$$\delta I = T_o \left(dS_{V.C.} + \sum s_{out} dm_{out} - \sum s_{in} dm_{in} + \frac{\delta Q_o}{T_o} + \sum \frac{\delta Q_k}{T_k} \right) \qquad \text{(Ec. 17)}$$

The exergy efficiency is defined as the relationship between the total exergy of preserved and the total exergy used in a process:

$$\xi = {}^{\dot{E}x_{out}}\!\Big/_{\dot{E}x_{in}} = 1 - {}^{\dot{I}}\!\Big/_{\dot{E}x_{out}} \qquad \text{(Ec. 18)}$$

Where "out" is understood by the net output or the "product", the "desired value" or "benefit", and the "in" is understood by "given", "used" or "delivered".

For the purposes of this research, the global exergy efficiency of the system has been defined the total exergy available in the cooling water generation versus the total radiant exergy captured, during a day of operation [6]. In order to analyze the meaning of these values of "efficiency", we must understand that the term "exergy efficiency" lacks of fixed value ranges that can be used for its interpretation; it means, this method of analysis is comparative, thus the greater the exergy efficiency is achieved, the lower the irreversibilities that are generated by the system and finally, the better the use of the exergy resources being used [14].

The percentages of efficiency depend on the initial point of analysis (reference point), therefore, the more specific with the origin of the exergy source or the greater exergy transfers are taken into account in the system, the efficiencies achieved will be lower, reflecting finally the irreversibilities that are generated by each processes or globally. For the exergy analysis presented in this paper, the system is being evaluated from its primary source of exergy (the sun), down to a final exergy output as hot or cold water for heating or cooling applications.

In order to evaluate the SHC system in different periods of the year, hours and mainly under the variation of cold demand pertaining to the summer season, a model in steady state was designed to obtain the energy and exergy balances, as well as the irreversibilities and efficiencies per component of the system, and finally the overall efficiency.

To determine the variation of the efficiency and the irreversibilities generated in the SHC system, the analysis was divided into two scenarios. These correspond to the operation with storage tanks, without phase change materials; and to the system operation with the storage tanks and the inclusion of phase change materials. Both scenarios correspond to the season that requires a generation of cold by the air conditioning system. These periods are an average day of the months of high, medium and low solar radiation, which were determined through the values previously found for the average amount of radiation received at the study area. In addition, each representative average day of the selected months were evaluated by hours, considering the work periods that the CIESOL has.

Finally, the phase change materials that corresponds to the second scenario under analysis were selected according to their melting temperatures and the temperature operating range of the cold and hot water storage systems. These correspond to the PCM Products Company [19], which works with hydrated salts in the air conditioning area (Table 2:).

Table 2: PCMs analyzed for the thermal energy storage in the SHC system [19]

	Hot PCM	**Cold PCM**
$\boldsymbol{Compound}$ **code** *(*hydrated salts*)*	$S70$	$S13$
$\boldsymbol{T_f}$ [°C]	70	13
$\Delta \boldsymbol{H_f}$ $[\boldsymbol{kJ \cdot kg^{-1}}]$	185	242
$\boldsymbol{\rho}$ $[\boldsymbol{kg \cdot m^{-3}}]$	1680	1515
$\boldsymbol{UA}$ $[\boldsymbol{W \cdot m^{-1} \cdot K^{-1}}]$	0.57	0.43
$\boldsymbol{Cp_{solid}}$ $[\boldsymbol{kJ \cdot kg^{-1} \cdot K^{-1}}]$	1.49	1.55
$\boldsymbol{Cp_{liquid}}$ $[\boldsymbol{kJ \cdot kg^{-1} \cdot K^{-1}}]$	2.10	1.90

3 Results

According to the collected information from the climatic characteristics of the Almeria region, the variations in cold demand by CIESOL and, finally, the application of the energy and exergy balances on the system, the following results were obtained.

3.1 Reference environment and cooling demand

The selected months of analysis correspond to May, September and August, as they are periods of low, medium and maximum solar radiation respectively, within the cooling demand season in CIESOL. The hours between 08h00 to 19h00, correspond to the work schedules that were established in the research center and represent the values where there is a cooling demand in the CIESOLs building. Subsequent values after 19h00 correspond to night hours, where the system enters into a storage mode of the accumulated energy during the daytime hours.

It can be observed from Figure 3 that during the summer season, August represents the warmest month with temperatures higher than 31 °C and minimum nights around 25 °C; on the other hand, May reflects minimum values up to 15 °C at the start of the day and maximums of 25 °C. These values determine the demand of cold in the building. Like the temperature data, May corresponds to the lowest intensities of solar radiation for the summer time. However, the differences between these months are not broad, which allows an advantage of the use of the solar source. The data shown in Figure 3, corresponds to values of direct solar radiation on the inclined plane of 30° of the solar collectors installed [11], these values differ from direct global radiation data on the Almeria location.

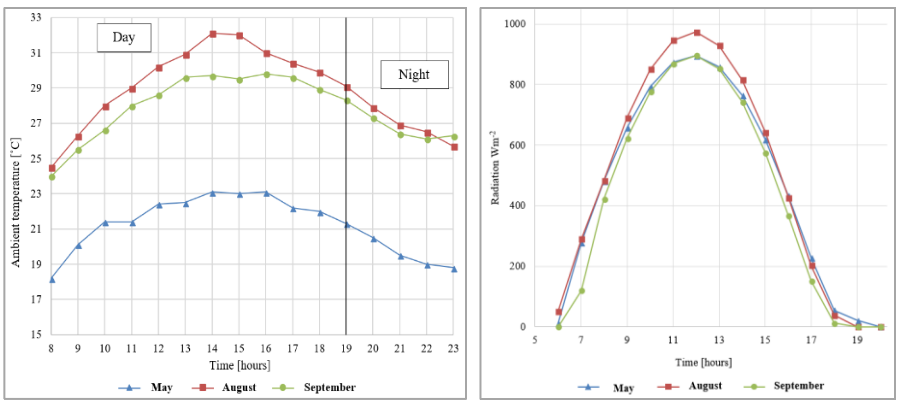

Figure 3: a) Average hourly variation of the ambient temperature in Almería b) Average hourly variation of the solar radiation in Almería

The cold demand values for the months of May, August and September, correspond to experimental data recorded by the CIESOL center during a period of three years, from 2010 to 2013. These cold demand hour values are the values registered at the output of the absorption chiller and are reflected in Figure 4, where the cold demand for an average day of the months under study can be observed. It is clarified that there is a rest period for the workers of the research center, from 14h00 to 16h00 pm, period in which there is still enough radiant useful and usable exergy by the system.

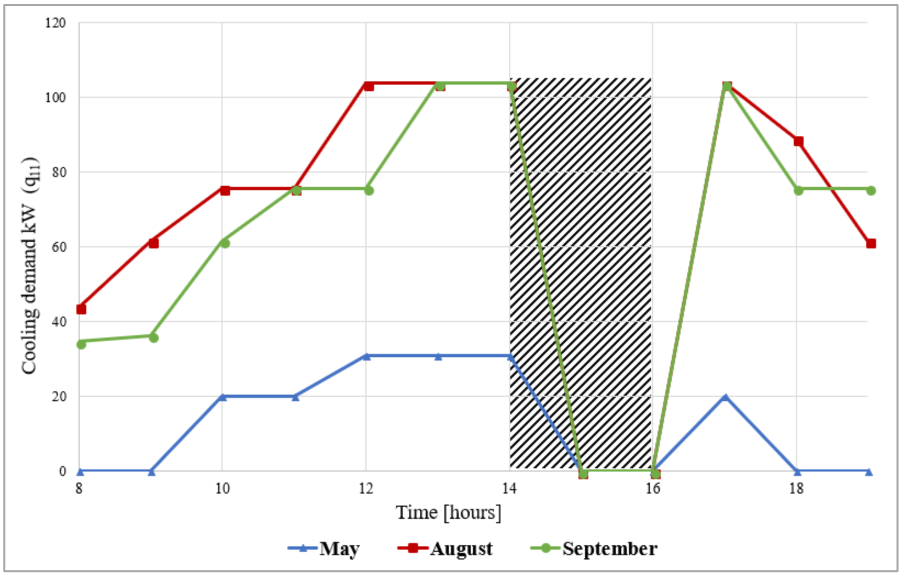

Figure 4: Daily average cooling demand for months of low, medium and maximum solar radiation

3.2 Efficiency and irreversibilities analysis of the SHC system by operating scenario

With the one-day operating data of the month of August, the thermodynamic values of each control point defined in the SHC system were calculated, and consequently the energetic and exergetic steady flow balances were made. The execution of these balance revealed the preliminary result of an experimental day, under a maximum operating capacity.

Table 3: Energetic balance

Process	Energy [kJ·s^{-1}]	Energy losses [kJ·s^{-1}]
Solar radiation	111.76	
Solar collector	62.61	49.15
Hot water storage tanks	39.56	23.05
Absorption chiller	N.D.	N.D.
Cold water storage tanks	-34.51	

*ND: Not determined

The application of the energy balance reveals an effect of the use of the First Law of Thermodynamics, which is the impossibility to contrast the thermal energy generated by the collectors, with the thermal energy absorbed for cooling resulting from the absorption chiller operation (it explains the N.D. marks of Table 3). As Asbik *et al* [20] mention, this law is insufficient to evaluate the energy performance of a thermal machine, because it does not take into account how the quality of the energy degrades (irreversibilities) in each component of the system, therefore it is only able to measure the amount of heat that can be stored or recovered. For this reason, the exergy analysis based on the Second Law of thermodynamics should be used to measure the quality of energy and then justify the thermodynamic imperfection of the real process.

Table 4: shows the values determined for the evaluation of the exergy transfer, which reflects the exergy availability of each process output and the losses generated in them. The results shown in both tables reveal different values, where the exergy that crosses the system is lower than the calculated energy. It is a characteristic of the exergy evaluation, because it considers the values of energy losses due to the system's components and the environment interaction [14]. Within the exergy balance, it was determined that the major losses are generated in the solar collectors and not in the absorption chiller where the generation of cold water occurs. This loss value corresponds to 94.7 $kJ \cdot s^{-1}$ of the 104.3 $kJ \cdot s^{-1}$ that enter to the solar collectors.

Table 4: Initial exergetic balance

Process	Exergy [$kJ \cdot s^{-1}$]	Exergy losses [$kJ \cdot s^{-1}$]
Solar radiation	104.33	-
Solar collector	9.58	94.75
Hot water storage tanks	5.89	3.69
Absorption chiller	3.52	2.37
Cold water storage tanks	2.66	0.86

The above exergetic balance can be better expressed through the efficiency values of Table 5:, where this efficiency was related to the inputs, outputs and recirculation flows of a control volume. The solar collectors' value shows the lowest exergy efficiency compared to the other components, with a percentage of only 9.17%. Another point to consider is the low overall efficiency determined, with a value of 6.54%.

Table 5: Exergy efficiency

Process	Exergy efficiency [%]

Solar radiation	-
Solar collector	9.17
Hot water storage tanks	89.04
Absorption chiller	59.83
Cold water storage tanks	88.90
Overall efficiency	6.54

All the previous analysis was translated into a mathematical model, which allows to determine hourly variations contemplated for the months under study and fulfill four fundamentals stages: data entry; construction of the thermodynamic characteristics of the 22 control points, according to the input data; execution of energy and exergy balances by control volume; and finally give the results of these balances (Table 6).

Table 6: Stationary flow model of the SHC system

Data

Hour	--				
$T_{environment}$ [°C]	T_0	--	**$T_{cold\ tank\ output}$ [°C]**	T_{12}	--
$T_{collector\ output}$ [°C]	T_1	--	**$m_{collector}$ [kg/s]**	m_1	--
$T_{hot\ tank\ output}$ [°C]	T_2	--	**$m_{hot\ tank}$ [kg/s]**	m_2	--
$T_{collector\ input}$ [°C]	T_3	--	**$m_{generator}$ [kg/s]**	m_4	--
$T_{generator\ input}$ [°C]	T_4	--	**$m_{cooling\ tower}$ [kg/s]**	m_6	--
$T_{generator\ output}$ [°C]	T_5	--	**$m_{evaporator}$ [kg/s]**	m_{10}	--
$T_{cooling\ tower\ output}$ [°C]	T_6	--	**$m_{cold\ tank}$ [kg/s]**	m_{12}	--
$T_{evaporator\ input}$ [°C]	T_{10}	--	**Irradiance [W/m^2]**	I	--

Thermodynamic properties of the system

State	Solution	$X_{(LiBr)}$ [%]	T [°C]	P [kPa]	$\dot{m}$ [kg/s]	h [kJ/kg]	s [kJ/kg·K]	ψ [kJ/kg]	Quality
0	H_2O	-	-	-	-	-	-	-	-
0	LiBr	52	-	-	-	-	-	-	-
0	LiBr	56	-	-	-	-	-	-	-

Solar collectors' energy balance

I_S [W/m^2]	-		
$\dot{E}_{sun}$ [kJ/s]	-		
Q_{sc} [kJ/s]	-		
h_1 [kJ/kg]	-	T_1 [°C]	-

Solar collectors' exergy balance

$\varepsilon_{sun,max}$ [kJ/kg]	-	$\dot{E}x_{radiant}$ [kJ/s]	-
$\dot{E}x_1$ [kJ/s]	-	$\dot{E}x_3$ [kJ/s]	-
$\dot{I}_{sc}$ [kJ/s]	-		
ξ_{sc}	-		

3.2.1 Scenario A: Solar heating and cooling (SHC) system with storage tanks

The application of the exergy balance revealed the global exergetic efficiencies achieved by the system for the three months under study in the storage operation mode (Figure 5). According to Hepbasli (2006), the values of the exergetic efficiency serve as a method of comparison between two or more systems, where a greater efficiency percentage results in a more efficient system in terms of management of the available energy resources and of minors irreversibilities generated throughout the transfer processes that are carried out [6].

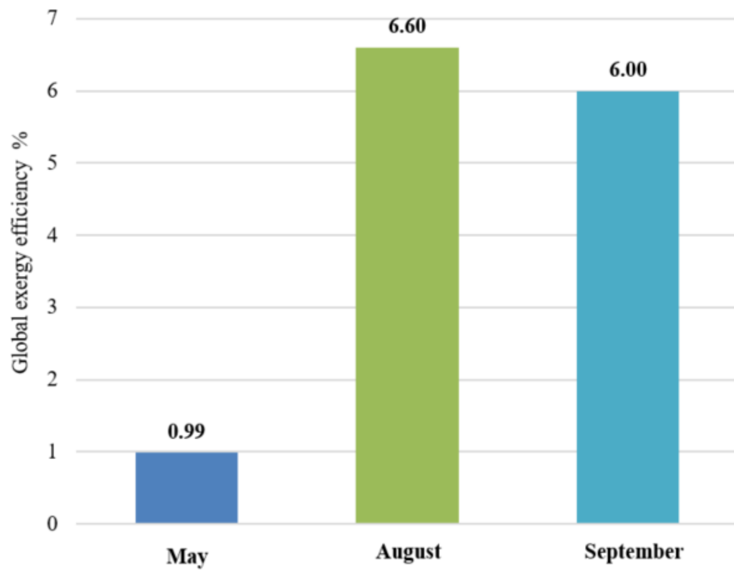

Figure 5: Variation of the global exergy efficiency for the SHC system with storage tanks

The obtained values correspond to the analysis of an operation day for the indicated months, with hourly intervals. In this sense, throughout the day, all the loading and unloading processes of the system have been considered, as well as the operation of the absorption chiller by the thermal energy storage tank during periods of low solar radiation. As we can see in Figure 5, August reached the highest exergy efficiency with a value of 6.60%, following September and May with values of 6.00% and 0.99% respectively.

These exergy efficiency values are related to the three main factors: the ambient temperature, the demand of chilled water and the direct solar radiation; since they determine the operation mode of the system itself. May represents the lowest values of ambient temperature and, therefore, the lowest demand for cold throughout a day. This directly affects the operating conditions of the system since it hardly works under optimal conditions, resulting in a low overall exergy efficiency (0.99%). In the other hand, August represents the maximum value reached by the system (6.6%), agreeing with the maximum registered temperatures, maximum solar radiation reached and greater cooling demand.

In order to have a better understanding of these results, a Grassmann diagram was made corresponding to an operation day of August, where all the irreversibilities generated during the operation of the refrigeration system in CIESOL are reflected (Figure 6).

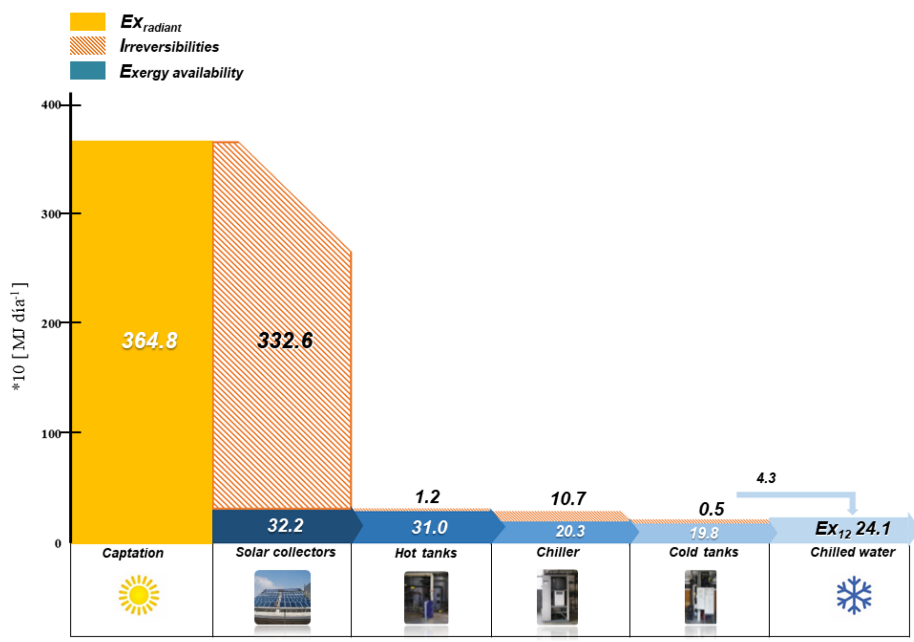

Figure 6: Grassmann Diagram. Irreversibilities during an average operation day of August expressed in MJ (SHC System with storage tanks)

Figure 6 shows that the total radiant exergy captured by the system during an average operation day on August was 3,648.3 MJ, where 3,326.3 MJ (90% of the exergy captured) is destroyed at the solar collectors, and only 322 MJ are transferred to drive the absorption chiller. The next control volume of greater irreversibilities corresponds to the absorption chiller with 107.1 MJ are destroyed. Finally, a useful exergy of 240.8 MJ is obtained as chilled water, representing only 6.6% of all the exergy captured. The Figure 6 also reflects an exergetic contribution to the generation of cold (42.8 MJ), which is a consequence of the adjacent equipment operation related to the SHC system such as pumps, valves, etc.

The fact that the major amount of irreversibilities is generated in solar collectors is an already known reality in the solar research field [21]. Regarding to all the solar potential that can be exploited, more than being an inefficient operation of the system itself, it is a technological inefficiency attributable to solar collectors. Likewise, it must be considered that the longer operating hours the system has, the greater are the exergy losses generated throughout the day.

The second component that generates irreversibilities in the SHC system corresponds to the absorption chiller. The studies carried out by Batlles & Rosiek [22] showed that the COP (Coefficient of Performance) of this component obtained by a First Law balance analysis, reached values between 0.33–0.8, that are considered optimal and "efficient" in terms of energy. In comparison, the exergy analysis of a LiBr simple effect absorption chiller [23] [10], revealed that despite the relatively high energy performance values achieved by this equipment, they have a low exergy efficiency, where the main reason is the large quantities of mass and heat flow transfers that occur in each component, which affect the overall efficiency of the system.

Other studies [10] also highlighted that the component that produced the greatest irreversibilities in the chiller corresponds to the generator, due to the temperature difference of the thermal energy source and the internal working temperature of the system. This same situation was reflected in the exergy analysis of the absorption chiller under study, where the global exergy efficiency values were registered between 20 - 59%, higher than those recorded in the cited study [10]. It is because the entry temperature generated by the solar collectors was lower than that used by the absorption system that works with superheated steam, thus the SHC system's absorption chiller represent a lower temperature difference between the thermal source and the internal working fluid.

3.2.2 Scenario B: Solar heating and cooling system (SHC) with storage tanks and phase change materials (PCMs)

In this second scenario, Figure 7 shows the overall exergy efficiency values determined for the months of May, August and September, which were 0.64, 6.57 and 5.58% respectively. Comparing these values of global exergy efficiency with the values obtained in the previous scenario, it can be observed that the global exergetic efficiencies are slightly lower. It does not necessarily mean that the system is acting more inefficiently because of the use of phase change materials in the cold and heat storage tanks, but that there is a greater amount of exergy accumulated in the storage tanks. Therefore, it can be stated that the installation of the phase change materials influences the operation of the SHC heating and cooling system, however, this is minimal.

The introduction of the PCMs in the cold and heat reserve tanks, leads to an increase in the thermal capacity of these tanks, thus achieving a greater capacity for accumulation and therefore higher performance [24]. The action mode of these

PCMs is based on the fact that once their environment reaches the melting temperatures of the materials, they absorb or release latent heat depending on external needs, acting as net reserves of exergy [1].

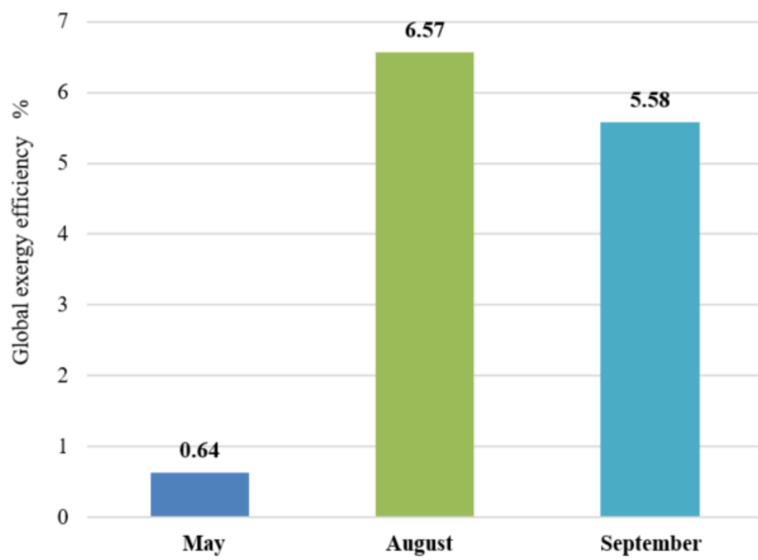

Figure 7: Global exergy efficiency variation for the SHC system with storage tanks and PCMs

The reason why the exergy efficiency of the system falls in this last scenario is due, on the one hand, to the fact that the introduction of these materials represents a new transfer of heat that occurs inside the storage tanks and, as we have seen before, the more heat transfers a system has, the greater irreversibilities are produced by it [14]. On the other hand, and the main reason for the reduction, is that the system is now producing an increase in the exit temperatures of the tank at the final delivery of the chilled water, resulting in a lower exergy delivered, which in fact has not been lost, but is accumulated in the tanks.

Figure 8 quantitatively reflects the amount of irreversibilities generated by the storage tanks, as well as the increase in the amount of exergy accumulated in them. In this figure, the irreversibilities generated by the solar collectors are not showed, as well as the incoming radiant exergy, in order to better observe the amount of irreversibilities generated in the other system´s components. And more importantly, it shows that a lower entry temperature in the absorption chiller produces a lower amount of irreversibilities (a situation that have been previously detailed). Finally, we can observe the strong potential of the PCMs to store exergy for the heat and cold reserves, being the heat tanks the site where greater amount of exergy is stored regarding their higher volumetric heat capacity [22].

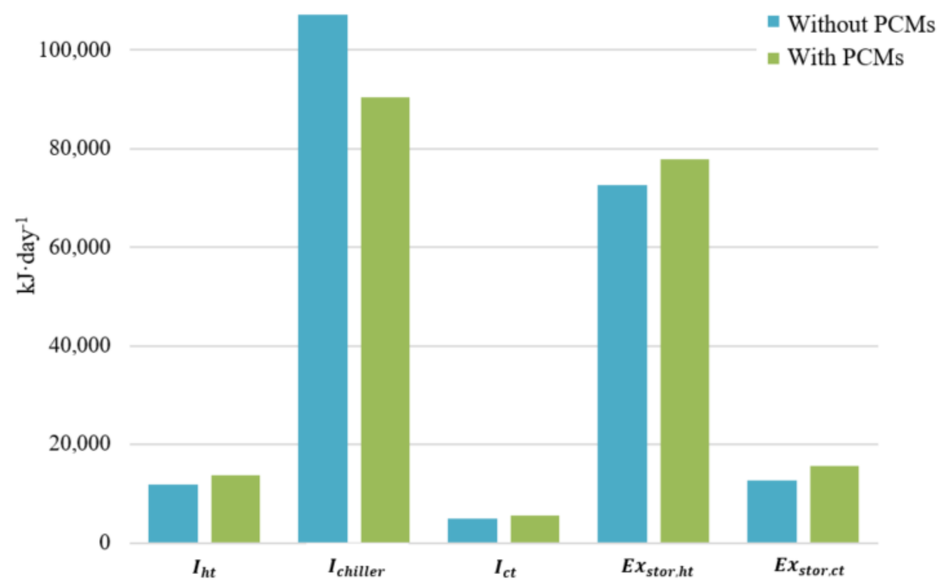

Figure 8: Total amount of irreversibilities in kJ·day-1, during an average operation day for the month of August (Scenario a and b)

Iht = Heat tanks irreversibilities; *Ichiller* = Absorption chiller irreversibilities, *Ict* = Cold tanks irreversibilities; *Ex stor,ht* = Exergy stored in the heat tanks; *Ex stor,ct* = Exergy stored in the cold tanks

Figure 9 consists of a Grassmann Diagram, where the irreversibilities of the cold storage tanks, as well as the solar collectors, are greater than those registered in the scenario A, but the irreversibilities of the absorption chiller diminish considerably due to the presence of the phase change materials. Both Figures, 9 and 10, demonstrate that, despite the introduction of the PCMs and the increase of the thermal energy capabilities, the irreversibilities of the system increase and therefore decrease the exergy efficiency. This is also because the components with the greater irreversibilities of the system have not been improved, and therefore the objectives of reducing the inefficiencies found in the system are not relevant.

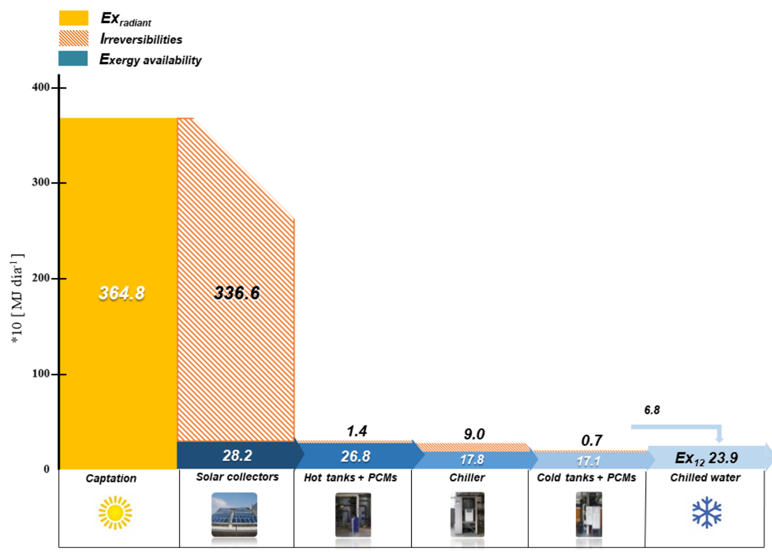

Figure 9: Grassmann Diagram. Irreversibilities during an operation day for the month of August expressed in MJ (SHC System with tanks and PCMs)

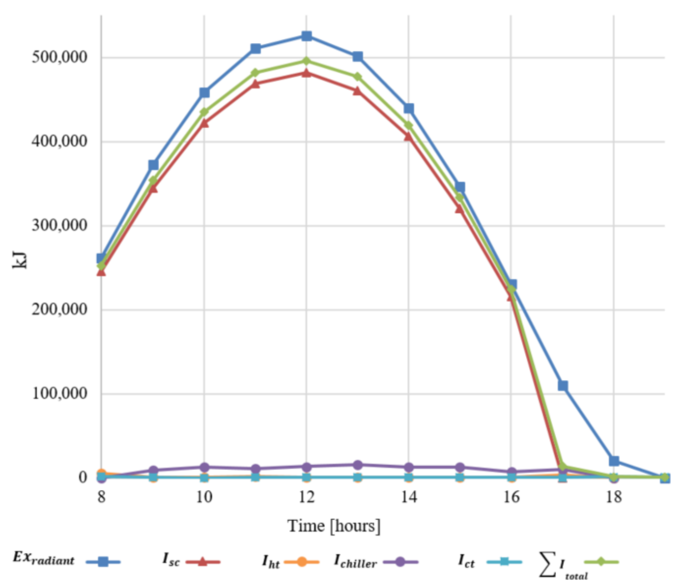

Figure 10: Hourly variation of the radiant exergy and the irreversibilities for an operation day of August (SHC system with storage tanks and PCMs)

Ex radiant = Radiant exergy*; Isc* = Solar collectors irreversibilities*; Ihbt* = Hot tanks irreversibilities; *Ichiller*= Chiller irreversibilities, *Ict* = Cold tanks irreversibilities; *Itot* = Global irreversibilities

3.3 Irreversibilities reduction proposal in the SHC system

As it was shown, the SHC system currently installed at CIESOL has a great potential to satisfy the cooling demand of the building. However, the introduction of the PCMs (one of the main elements of study) does not increase the exergy efficiency of the system but decreases it by storing a greater amount of exergy in the cold tanks. The exergy analysis showed that, regardless of the scenario (A or B), the solar collectors generate the greatest irreversibilities (around 90% of the entire generation) followed by the absorption chiller, the storage tanks and finally the phase change materials. Therefore, the irreversibilities reduction proposal in order to obtain a more exergy efficient system must consider in first place the technology used for collecting the solar exergy.

A study conducted by Saitoh *et al* [25], focused on the energy and exergy efficiency evaluation of solar thermal collectors and photovoltaic panels, revealed that despite the known energy performance of solar collectors, about 46.2% (Table 7), the exergy efficiency results reached values of just 4.4% for that type collectors. On the other hand, the photovoltaic panels that usually show 10% energy efficiency, the study showed that its exergy efficiency was higher, reaching a value of 11.2%, higher than the exergetic efficiencies reached by the solar collectors.

Table 7: Energy and exergy efficiency evaluation for solar collector and photovoltaic modules [24]

Efficiency	Solar collectors	Photovoltaic modules
Energy performance (η, %)	46.2	10.7
Exergy efficiency (ξ, %)	4.4	11.2

Table 8: Energy and exergy efficiency evaluation for solar collector and photovoltaic modules currently installed at CIESOL

Efficiency	Solar collectors	Photovoltaic modules
Energy performance (η, %)	59.29	14.20
Exergy efficiency (ξ, %)	8.80	15.00

An energy and exergy evaluation of the solar collectors currently installed at CIESOL showed that the exergy efficiency values reached by them were 8.80% (Table 8), and an energy performance of 59.24%, similar values to those cited by Saitoh *et al* [25]. In contrast, the same energy and exergy analysis was executed for the photovoltaic panels also currently installed at CIESOL, which reached an exergy efficiency of 15%.

Comparing both solar technologies (thermal collectors and PV panels), it can be seen the strong limitation represented by the analysis of the first law of thermodynamics, which analyzes the transformation of energy but fails to measure the amount of exergy that is lost [26]. Therefore, despite the performance values that are usually handled, photovoltaic panels represent a better solar technology than the solar collectors, in exergetic terms, for the purpose presented here. Thus, there is indeed a technological solar option that allows a better use of solar resources.

An alternative proposal to the current solar heating and cooling system is presented below, based on the use of photovoltaic modules as the main source of electricity supply, which drives a cooling system to meet the demand of the CIESOL center. This proposed system is based on components currently installed at the building, where the PV panels are used to cover the electrical demand of the center and the vapor compression cycle is used as a back-up refrigeration system in case of failures (Figure 11 a and b).

Figure 11: a) Photovoltaic panels b) Vapor compression cycle (Ciatesa) currently installed at CIESOL [9]

The proposed system for the cooling demand of CIESOL consists of 47 Artesa A-222P photovoltaic modules, with an electrical generation capacity of 10.4 kWp and an inclination of 22° to the south. This energy is converted through inverters Cycle 3000 and supply the necessary energy to a vapor compression cycle CIATESA WE 360, which uses R-410a as refrigerant and finally covers the cooling demand of the center (Figure 12).

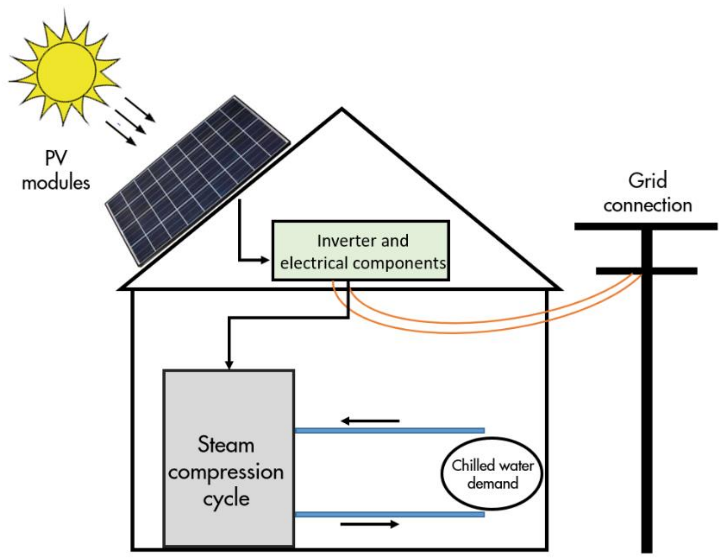

Figure 12: Heating and cooling system proposal supplied by solar electric energy

The first difference between the SHC system based on PV panels and the solar collector system, is the quantity of components necessary for the generation of cold. As shown in Figure 1, the amount of principal and complementary components that are needed to meet the current refrigeration demand of the center is greater compared to that shown in Figure 13:. This is mainly due to the versatility that represents the electrical energy generation [26], since it is easily consumed, stored in batteries or directly injected to the local electrical connection. The overall exergy efficiency achieved for an average day of August was 9.14%, a value greater than the maximum global exergetic efficiency reached by the solar collector system, with a value of 6.6% for scenario A (Figure 5). This represents an increase of 38.5% in the overall efficiency.

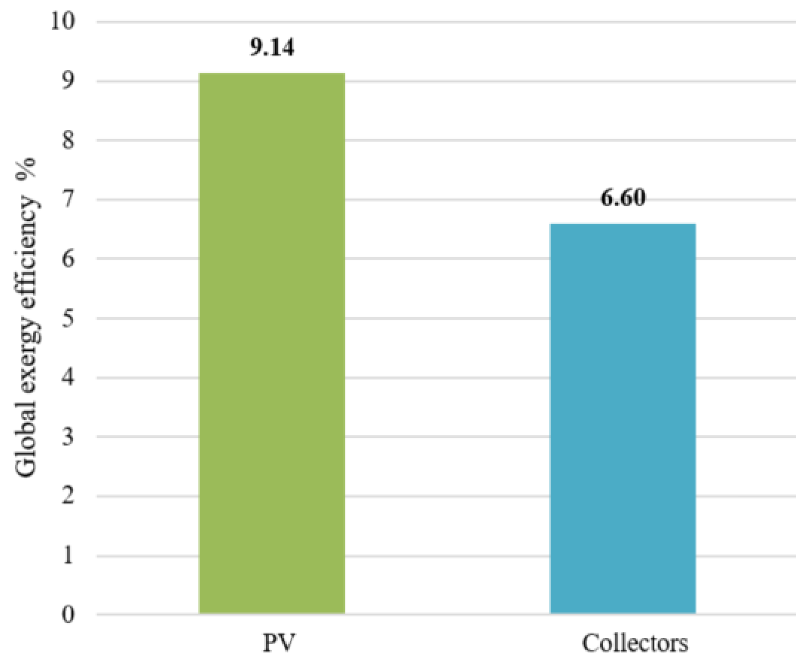

Figure 13: Global exergy efficiency comparison between the solar thermal collectors and PV systems during an operational day of August

The reduction of irreversibilities is based on two main points: first is related to the greater exergetic efficiency achieved by the PV panels and second to the least amount of exergy losses due to the minor components necessary for the production of cold [14].

Figure 14 shows the corresponding Grassmann Diagram for the proposed solar cooling system. This shows that despite the increase in the exergy efficiency achieved by photovoltaic panels, solar exergy collections remains the highest irreversibility generated in the system, followed by the vapor compression cycle or heat pump. However, the presence of fewer components has a positive effect on the overall exergy efficiency of the system. It can also be seen that there is an important contribution of 39.1 MJ to the system, due to the recirculation of flows and the use of pumps.

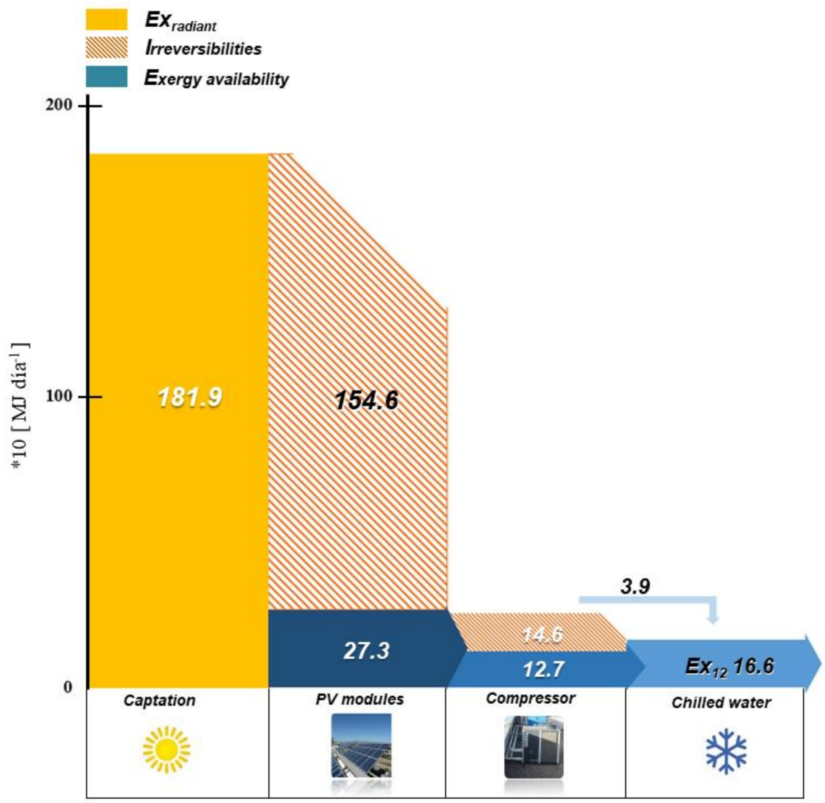

Figure 14: Grassmann Diagram. Irreversibilities during an average operational day of August expressed in MJ (Solar cooling system proposed)

Regarding the economic investment on both systems, the first one corresponds to the solar collector system, occupies an area of 160 m² and has an investment of € 150,000 with an operation and maintenance costs of € 1,500 per year according to Batlles & Rosiek [21], where the most expensive equipment was the absorption chiller. In contrast, the proposed system powered by photovoltaic panels and using the same economic approaches of the prior system, could use an area of 80 m² with € 82,000 investments and an operation and maintenance cost of € 820 per year, demonstrating that the fixed and variable investment of the proposed system is significantly lower than the current solar thermal system.

Finally, despite the greater exergy efficiency achieved by the proposed solar heating system (powered by PV energy) and its lower investment cost, a drawback of the use of vapor compression cycles is due to the need of refrigerants, such R-410A, even if it is considered one of the last generation refrigerants because it does not contain chlorine and bromine compounds and does not contribute to the reduction of the ozone layer; it is considered a powerful greenhouse gas [27].

4 Conclusions

A fundamental concept of Efficiency is necessary to properly analyze and optimize any SHC system, due to the limitation of the Fist Law of thermodynamics. This investigation showed that the maximum global exergy efficiency obtained by the solar heating and cooling system currently installed at CIESOL is 6.6 %. It also revealed that most of the solar radiation exergy is lost at the thermal collectors, followed by the absorption chiller. Also, contrary to what was expected, the introduction of the PCMs do not represent a significant improvement in the efficiency of the system. Nevertheless, PCM systems can be used to improve the amount of exergy that can be stored; therefore, it can be used at other moments of the day and can be an alternative to storing the solar exergy into batteries, especially for exergy saved as cold. An analysis should be done if it is convenient to save exergy in cold tanks rather to save exergy in hot tanks as it is done at present at CIESOL.

To conclude, a different solar cooling system was proposed in order to reduce the irreversibilities generated by the system. It consists on a photovoltaic system and a vapor compression cycle, where it was found that PV modules are more efficient than the thermal collectors, with a global exergy efficiency of 9.14%, which represents an increase of 38.5% in the overall efficiency. This system could also allow to save exergy directly in cold tanks rather than in hot tanks and improving the global efficiency of the system.

5 Acknowledgments

This work was supported by the ERANET-LAC CONICIT/PCI/ELAC2015/T06-0988 project. And the partial support of the CONICYT/FONDAP N°15110019 project in this research.

Bibliographic References

[1] H. Shabgard, L. Song y W. Zhu, «Heat transfer and exergy analysis of a novel solar-powered integrated,» Energy Conversion and Management, nº Heat transfer and exergy analysis of a novel solar-powered integrated, pp. 121-131, 2018.

[2] U.S. Energy Information, "Residential Energy Consumption Survey (RECS) – Data," [Online]. Available:

https://www.eia.gov/consumption/residential/data/2009/index.php?view=consumption. [Accessed 2018 December 18].

[3] International Energy Agency, "Key world energy statistics," 2017. [Online]. Available: https://www.iea.org/publications/freepublications/publication/KeyWorld2017.pdf. [Accessed 18 December 2018].

[4] T. S. Ge, R. Z. Wang, Z. Y. Xu, Q. W. Pan, S. Du, X. M. Chen, T. Ma, X. N. Wu, X. L. Sun y J. F. Chen, «Solar heating and cooling: Present and future development,» Renewable Energy, vol. Accepted manuscript, 2017.

[5] F. Esposito , A. Dolci, G. Ferrara, L. Ferrari y E. A. Carnevale, «A case study based comparison between solar thermal and solar electric cooling,» Energy Procedia 81, pp. 1160-1170, 2015.

[6] A. Hepbasli, «A key review on exergetic analysis and assessment of renewable energy resources for a sustainable future,» Renewable and Sustainable Energy Reviews, pp. 593-661, 2006.

[7] A. Bejan, G. Tsatsaronis y M. Moran, «Thermal design and optimization,» New York: Wiley, 1996.

[8] S. Anand y S. K. Tyagi, «Exergy analysis and experimental study of a vapor compression refrigeration cycle,» Journal of Thermal Analysis and Calorimetry. 110, pp. 961-971, 2012.

[9] S. Rosiek y F. Batlles, «Performance study of solar-assisted air-conditioning system provided with storage tanks using artificial neural networks,» International Journal of Refrigeration, pp. 1446-1454, 2011.

[10] F. Zadeh y N. Bozorgan, «The Energy and Exergy Analysis of Single Effect Absorption Chiller,» Advanced Design and Manufacturing Technology , pp. 100-109, 2011.

[11] PVGIS, "Photovoltaic Geographical Information System (PVGIS)," [Online]. Available: http://re.jrc.ec.europa.eu/pvgis/. [Accessed 10 February 2018].

[12] Agencia Estatal de Meteorología, AEMET, "AEMET," [Online]. Available: http://www.aemet.es/es/portada. [Accessed 16 March 2018].

[13] SiAR, «Sistema de Información Agroclimática para el Regadío,» 12 Enero 2017. [En línea]. Available: http://eportal.mapama.gob.es/websiar/SeleccionParametrosMap.aspx?dst=1.

[14] K. Wark y D. Richards, Termodinámica, Sexta ed., Madrid: McGRAW-HILL, 2001.

[15] D. Cabrera y J. Gil, Sistemas Solares, para el calentamiento de agua, Cochabamba, 1996.

[16] J. Gonzáles, Energías renovables, Barcelona: Reverté, 2009.

[17] S. Kalogirou, Solar Energy Engineering - Processes and Systems, Academic Press, 2014.

[18] R. Petela, «Energy of heat radiation,» J. Heat Transfer, pp. 187-192, 1964.

[19] Phase Change Material Products Limited, "Products," [Online]. Available: http://www.pcmproducts.net/. [Accessed 18 February 2017].

[20] M. Asbik, O. Ansari, A. Bah, N. Zari, A. Mimet y H. El-Ghetany, «Exergy analysis of solar desalination still combined with heat storage system using phase change material (PCM),» Desalination, pp. 26-37, 2015.

[21] J. M. De Juana, A. De Francisco, J. Fernandez, F. Santos, M. Á. Herrero y A. Crespo, Energías Renovables para el Desarrollo, Madrid: Thomson, 2003.

[22] F. Batlles y S. Rosiek, «Renewable energy solutions for building cooling, heating and power system installed in an institutional building: Case study in southern Spain,» Renewable and Sustainable Energy Reviews, pp. 147-168, 2013.

[23] M. Azhar y M. Altamush Siddiqui, «Exergy analysis of single to triple effect lithium bromide-water vapour,» Energy Conversion and Management, nº 180, pp. 1225-1246, 2019.

[24] G. Lavinia, «Thermarl Energy Storage with Phase Change Material,» pp. 75-98, 2012.

[25] H. Saitoh, Y. Hamada, H. Kubota, M. Nakamura, K. Ochifuji, S. Yokoyama y K. Nagano, «Field experiment and analyses on a hybrid solar coleector,» Applications Thermal Energy, pp. 23-105, 2003.

[26] F. Bayrak, N. Abu-Hamdeh, K. A. Alnefaie y H. F. Oztop, «A review on exergy analysis of solar electricity production,» Renewable and Sustainable Energy Reviews, pp. 755-770, 2017.

[27] ASHRAE, «Heating, Ventilating, and Air-Conditioning Systems and Equipment,» de ASHRAE Handbook - Fundamentals, knovel, 2013.